Morphologic indicators for severe central nervous system defects in genetically engineered mouse embryos

Reissig LF[1], Moghaddam AS[1], Prin F[2], Wilson R[2], Galli A[3], Tudor C[3], White JK[3], Geyer SH[1], Mohun TJ[2] and Weninger WJ[1]

[1]Division of Anatomy, MIC, Center for Anatomy and Cell Biology, Medical University of Vienna, Vienna, Austria
[2]The Francis Crick Institute, London, United Kingdom
[3]Wellcome Trust Sanger Institute, Wellcome Genome Campus, Cambridge, United Kingdom

Objective

In researching human central nervous system (CNS) disorders the identification of appropriate knockout (KO) mouse models is essential [1]. As many KO-lines produce pre- or perinatally lethal homozygous offspring, their analysis rests upon phenotyping accessible embryonic stages [2]. This is complicated by the fact that many mouse lines show highly variable penetrance of phenotypes [3], wherefore severe phenotypes, causing early lethality are easily missed and large numbers of embryos have to be bred and harvested. To facilitate reduction of numbers and to ensure that early lethal malformations are not missed, we aimed at identifying mild morphologic abnormalities that have the potential to serve as indicators for low penetrant CNS defects (Fig.1) in genetically modified mouse lines.

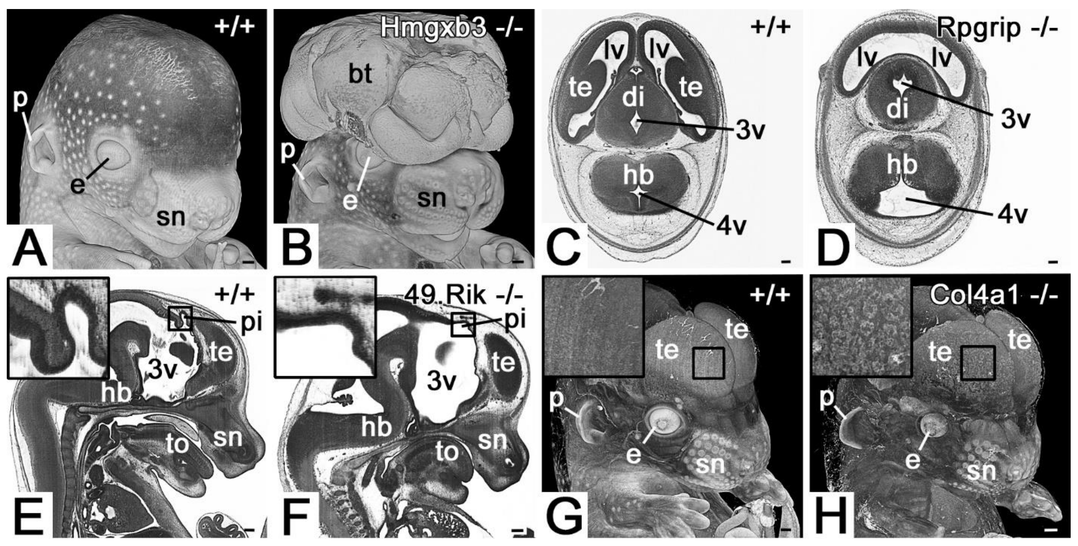

Fig 1: Selected malformations of the central nervous system, associated with hypoglossal nerve abnormalities. **A, B**. Exencephaly in a Hmgxb3 null mutant (B) **C, D**. Holoprosencephaly in a Rpgrip null mutant (D). Axial HREM section. The lateral ventricles (lv) are in direct continuation. **E, F**. Abnormal morphology of pineal gland vesicle (pi) in a 4933434E20Rik null mutant (F). Sagittal re-section through HREM data. **G, H**. Abnormal architecture of the telencephalic cortex in a Col4a1 null mutant (H). Abr: p, pinna; e, eye; sn, snout; bt, brain tissue; 3v, 3rd ventricle; 4v, 4th ventricle; di, diencephalon; hb, hindbrain; te, telencephalon; to, tongue; Scalebars: 250 µm, Modified from [6]

Material and Methods

Approximately 500 homozygous null mutant embryos of 81 single gene KO-lines were harvested at embryonic day 14.5 and digital volume data were created using High-resolution episcopic microscopy (HREM) [4]. Employing the data stacks and volume rendered computer models the phenotypes of the embryos were systematically analysed following a standardised protocol [5].

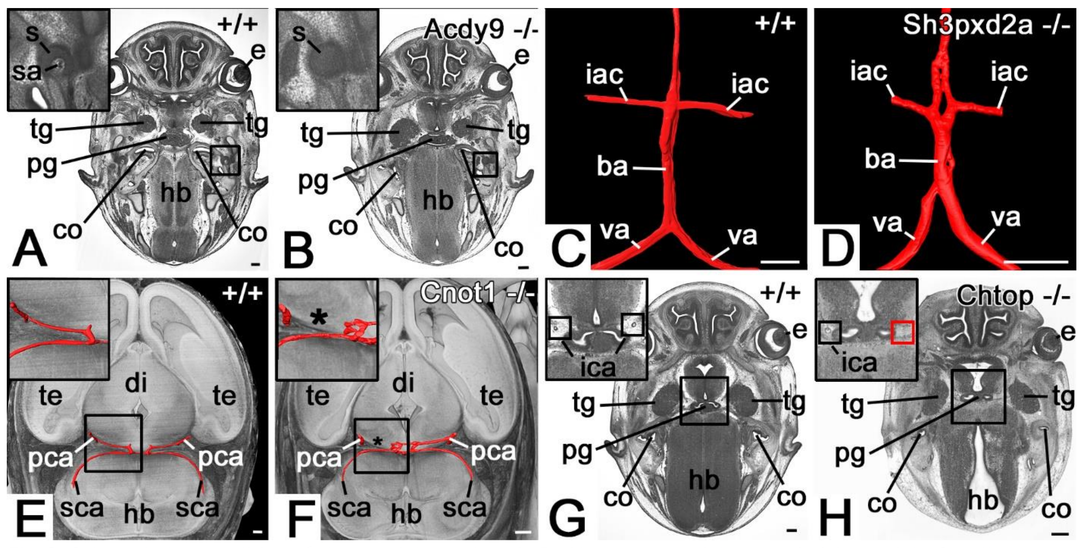

Fig 2: Selected abnormalities of the cranial arteries: **A, B**. Absent stapedial artery (sa) in an Adcy9 null mutant (B). Axial HREM section. **C, D**. Abnormal basilar artery morphology in a Sh3pxd2a null mutant (D). 3D surface model (red) of basilar artery (ba), vertebral arteries (va) and inferior anterior cerebellar arteries (iac) from dorsal. **E, F.** Absent segment of posterior cerebral artery (pca) in a Cnot1 null mutant (F). Surface model (red) of the posterior cerebral and superior cerebellar arteries (sca) and their connections in the context of an axially sectioned volume model of the head from superior. The asterisk indicated where the missing segment is to be expected. **G, H.** Absence of right sided parasellar internal carotid artery (ica) in a Chtop null mutant (H). Axial HREM section. Red box in H indicated the expected position of the artery. Abr: s, stapes; e, eye; tg, trigeminal ganglion; pg, pituitary gland; co, cochlea; hb, hindbrain, te, telencephalon; di, diencephalon; Scalebars: 250 µm. Modified from [6]

Results

First analysis identified two promising indicator candidates. Abnormal morphology and topology of head arteries (Fig. 2) and hypoglossal nerve (HGN) abnormalities (absent, thin, and abnormal topology) (Fig. 3). Both are frequently associated with the full spectrum of morphological CNS defects. Statistical analysis however confirmed a significant correlation with CNS defects only for HGN abnormalities (Fig. 4).

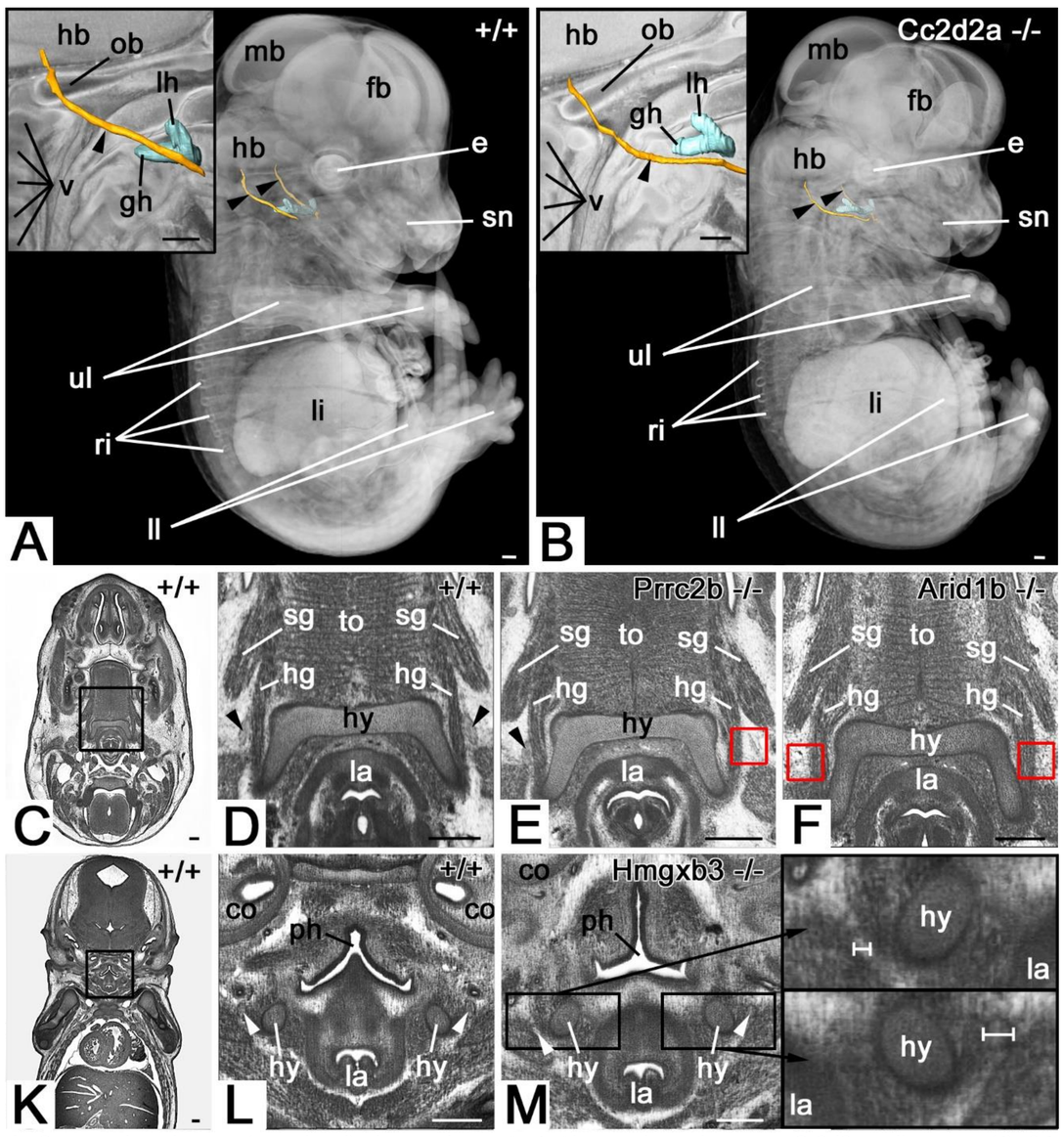

Fig 3: Hypoglossal nerve (arrowhead) abnormalities. **A, B.** Abnormal topology in a Cc2d2a null mutant (B). 3D surface models of hyoid bone (turquoise) and hypoglossal nerve (orange) in context of semi-transparent and median sectioned (inlay) volume models from right. **C-F.** Absent nerve at the level of hyoid bone (hy) in axial HREM sections of Prrc2b (E) and Arid1b (F) mutants. Red boxed areas indicate positions where the nerve is missing unilaterally (E) and bilaterally (F). **K-M**. Unilateral thinning of the nerve in coronal re-sections through HREM data of a Hmgxb3 null mutant (M). Note the different thickness (white scalebars) of the thinned nerve (top inlay) compared to the normal nerve (bottom inlay) Abr: fb, forebrain; mb, midbrain; hb, hindbrain; lh lesser horn of hyoid bone; gh, greater horn of hyoid bone; ob, occipital bone; v, vertebra; e, eye; sn, snout; ri, ribs; li, liver; ll, lower limb; ul, upper limb; co, cochlea; sg, styloglossus muscle; hg, hyoglossus muscle; la, larynx; to, tongue; ph, pharynx; Scale bars, 250 µm. Modified from [6]

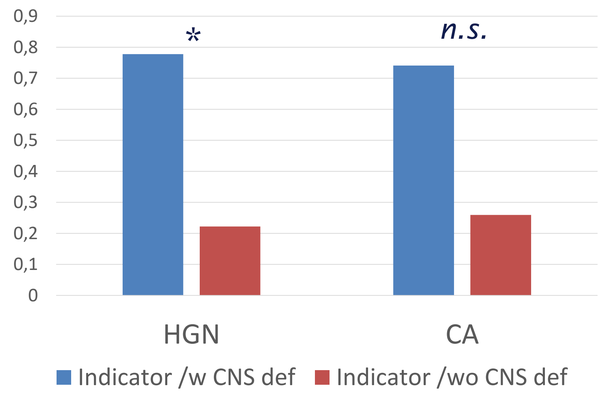

Fig 4: Bar-Plot of the percentages of KO-lines showing abnormalities of an indicator structure (hypoglossal nerve (HGN), cranial arteries (CA)) that do (blue) and do not (red) also feature CNS defects. *=p<0.05, n.s.= not significant

Conclusion

These results demonstrate that KO-lines showing HGN abnormalities are also likely to produce CNS defects. Therefore the HGN can be used as indicator to identify KO-lines featuring low penetrant CNS malformations.

References & Funding information

[1] Brown, S. D. M. & Moore, M. W. The International Mouse Phenotyping Consortium: past and future perspectives on mouse phenotyping. Mamm. Genome 23, 632–640 (2012)
[2] Mohun, T. et al. Deciphering the Mechanisms of Developmental Disorders (DMDD): a new programme for phenotyping embryonic lethal mice. Dis. Model. Mech. 6, 562–566 (2013)
[3] Wilson, R. et al. Highly variable penetrance of abnormal phenotypes in embryonic lethal knockout mice. Wellcome Open Res 1, 1 (2016)
[4] Weninger, W. J. et al. High-resolution episcopic microscopy: a rapid technique for high detailed 3D analysis of gene activity in the context of tissue architecture and morphology. Anat. Embryol. 211, 213–221 (2006)
[5] Weninger, W. J. et al. Phenotyping structural abnormalities in mouse embryos using high-resolution episcopic microscopy. Dis. Model. Mech. 7, 1143–1152 (2014)
[6] Reissig, L. F. et al. Hypoglossal Nerve Abnormalities as Biomarkers for Central Nervous System Defects in Mouse Lines Producing Embryonically Lethal Offspring. Front. Neuroanat. 15, 625716 (2021)

This work was supported by the Wellcome Trust (100160) and the Francis Crick Institute, which receives its core funding from Cancer Research UK (FC001117), the UK Medical Research Council (FC001117), and the Wellcome Trust (FC001117).